Physical and mechanical properties of clay–sand mixes to assess the performance of earth construction materials

Elsa Anglade, Jean-Emmanuel Aubert, Alain Sellier, Aurélie Papon

Physical and mechanical properties of clay–sand mixes to assess the performance of earth construction materials

Elsa Anglade, Jean-Emmanuel Aubert, Alain Sellier, Aurélie Papon

LMDC, Université de Toulouse, INSA/UPS Génie Civil, 135 Avenue de Rangueil, 31077 Toulouse cedex 04 France

Abstract

The reduction of CO_2 emissions has become an important parameter in the choice of construction materials. Earth guarantees a low environment impact due to the reduced need of energy for its processing and transportation and also provides natural hygrothermal comfort. To facilitate the design of earthen constructions, the development of models is necessary. This paper aims to provide a database of experimental results that could be easily used for developing models based on the competition between positive effect of capillary pressure on material cohesion and negative effect induced by matrix shrinkage restrained by aggregates. Mechanical and thermal tests were carried out on three reconstituted soils composed of pure kaolinite and three contents of fine sand (0, 30 and 60%), as well as different water content configurations (fabrication water content and after drying at 50% RH). The thermal properties analyzed included thermal conductivity and specific heat capacity. The mechanical properties studied encompassed the tensile (three-point bending test) and compressive strengths, Young's modulus and Poisson's ratio (using video correlation). Moreover, an original test was developed for measuring sample shrinkage during drying. Specifically, the results clearly showed that while shrinkage is divided by 5 for the maximal sand content, tensile strength is reduced by half. Therefore, these results allow to assess the balance between benefices and disadvantages of capillary pressure induced by clay drying on earth construction materials, which is of first interest to assess cracking risk in a structure.

Keywords: earthen materials, mechanical properties, thermal properties, reconstituted soil

1 INTRODUCTION

The construction sector ranks among the largest economic activities in the world, while also being the largest consumer of energy. According to the French Ministry of Ecology, Sustainable Development and Energy, residential and commercial buildings were responsible for 44% of the French energy consumption in 2011 [1]. Several solutions have been explored to limit the energy consumption of construction activities, including the use of materials with a low environmental impact.

Earth has been used as a construction material for thousands of years. According to Minke [2], approximately 30% of the world's population was living in earth buildings in 2009. Earth is locally available in large quantities and guarantees a low environmental impact due to the reduced transport of the material and the low energy needed for its transformation and recyclability. Earthen materials are also well-known for their high capacity for storing humidity and heat. According to several authors [3]–[6], the hygroscopic properties of earth allow to regulate the relative humidity of a building and to sustain a comfort humidity level without using a ventilation system. The thermal conductivity of earth, which is ranging from 0.3 to 1 W/(m.K) [7], [8], is not low enough to consider this material to be a good insulator. However, Jeannet and Pollet [9] demonstrated how the thermal inertia of earth can maintain a comfort temperature inside a building below 25 °C for several weeks while the external temperature exceeds 30 °C.

Despite the good thermal and hygroscopic properties of earth, its use as a construction material is limited by the lack of regulations and the high variation of mechanical properties that depend on the location of the construction. In order to deem an earthen material suitable for construction, a long experimental campaign is required [10]. To reduce the length of this process and thus facilitate the choice of earth as a material of construction, it could be interesting to use a model based on homogenization procedures that is able to predict the mechanical and thermal properties of a soil according to its composition. This model would be able to determine the suitability of an earth to be used as a construction material. To develop such a model, a complete database of the properties of soils with different compositions would be necessary.

Numerous experimental studies have been undertaken on earthen materials to determine their mechanical and thermal properties. Compressive strength, Young's modulus and tensile strength have all been determined for many soil compositions, seeking to assess the mechanical properties of earth. To explore compressive strength, tests have been made on samples obtained with different methods and in various shapes and sizes, Miccoli et al. [11] analyzed cob samples, Morel et al. [12] tested compressed blocks and Avila et al. [13] contributed an exhaustive literature review of experimental campaigns focused on unstabilized rammed earth. The results are rather heterogeneous, with the compressive strength ranging from 0.5 MPa to 4 MPa, depending on the testing procedure and the composition of the material. Young's modulus is typically measured as the slope of the elastic part of a stress-strain curve [14]–[18]. However, the method of measurement of the strain of the sample can differ from one study to another. For example, Toufigh et al. [16] and Kosarimovahhed et al. [17] calculated the strain from the displacement of the platen of the press during a compressive test, while Champire [18] measured the strain through video correlation and Linear Variable Differential Transformer (LVDT) placed on the sample during a triaxial test. These different approaches have led to a large dispersion (60–1000 MPa) of Young's modulus values available in the literature. As for the tensile strength, few authors have measured it; most have used the Brazilian test, obtaining

values between 0.1 and 0.5 MPa [11], [16], [19]–[21]. These different mechanical tests have highlighted the fact that earth composition and the fabrication methods have a substantial impact on the results.

Moreover, the study of Bui et al. [22] demonstrated the relevance of water content and type of clay on the mechanical properties of earth. Earth is mainly composed of clay, sand and water. Each type of clay reacts differently in the presence of water, which would have an impact on the performance of the material. The mechanical results largely depend on composition, method of fabrication and testing procedure. If experimental data are to be used in a homogenization procedure, all these parameters must be thoroughly examined.

Many authors have measured the thermal properties of earth. For instance, Laurent [23] proposed a relation between thermal conductivity and earth density, having determined the thermal conductivity of eleven soil compositions. This relation has been questioned by Hall and Allinson [24], who demonstrated that density is not the only factor affecting thermal conductivity. Laurent [23] also highlighted a link between the water content of earth and thermal performance.

Even though numerous experimental campaigns have been carried out to this day, as illustrated in the literature review of Fabbri et al. [25], it is difficult to find a soil for which the entire composition is known, including the fabrication water content and the type of clay, and for which its mechanical and thermal properties have been measured. Furthermore, most studies have only analyzed mechanical or thermal properties separately. This study proposes a complete experimental campaign on specific reconstituted soils, including mechanical and thermal tests. For reasons of applicability of homogenization methods, a material with a clear difference of scales between the matrix constituents and the aggregates is required. Moreover, a narrow sand distribution is also needed to assume that the sand grains have the same size in the model. All the parameters which can influence the properties of earth, such as type of clay, clay content or water content, should be well known. Real earthen materials usually do not present all these characteristics. That is why this study on reconstituted soils is proposed.

In a first part, this article details the materials and procedures used in the experimental campaign. A second part describes the results, compares them to those found in the literature and finishes with a discussion of the results. A final part presents the conclusion and perspectives of this work.

2 MATERIALS AND PROCEDURES

2.1 Materials

The material used in this study is a reconstituted soil composed of clay, sand and water in different proportions. Clay and sand were carefully selected to create a material that reacts with water as little as possible and that can be easily modeled.

Clay is a material that can easily transition from a viscoplastic state to a brittle state in function of its water content. In earth construction, clay ensures the cohesion of the material and the cohesion between sand grains in particular. For this reason, a minimum of clay content is required to guarantee an adequate building material. Clay has a sheet-like structure where the surface properties of the sheets influence the organization and shape of the particles and their interaction with water [26], [27]. Expansive clays, such as smectites, have significant surface charges, which facilitates the occurrence of water between the sheets. This type of clay can induce important variations of volume, swelling or shrinkage in the presence of water, which can result in cracking when used as a construction material. Kaolinite, on the other hand, undergoes few surface charges and is a clay with relative low reactivity to water.

In this study, we decided to use the less hydro-sensitive clay, the kaolinite, to limit volume variation of the samples due to water content. A pure commercial sample of kaolinite was used (supplier specifications: >99% kaolinite, real density = 2.6 $g.cm^{-3}$). The grain size distribution (Fig 1) was determined by using sedimentometry in accordance with the NF EN ISO 17892-4 standard [28]. The chemical composition of kaolinite given by the supplier is detailed in Table 1.

If the sand grains are to be considered as inclusions, as per the homogenization theory, the size of the grains needs to be several orders greater than the clay particles. The silica sand selected for the samples has a relatively uniform grain size (200–400 µm; Fig 1) and is approximatively ten times bigger than the clay particles. While this particle size distribution does not match the distributions recommended by several guidelines [10], [29] since the sand grains are quite small, it complies with the matrix-to-inclusion difference of scale required to test homogenization procedures. As the particle size distribution will affect the mechanical properties of this reconstituted soil, differences between the mechanical properties of real soils and the one analyzed in this paper might exist. The chemical composition of sand is shown in Table 1 (dry bulk density = 1.55 $g.cm^{-3}$, real density = 2.6 $g.cm^{-3}$). Its water absorption (2.9%) was measured in accordance with the NF EN 1097-6 standard [30].

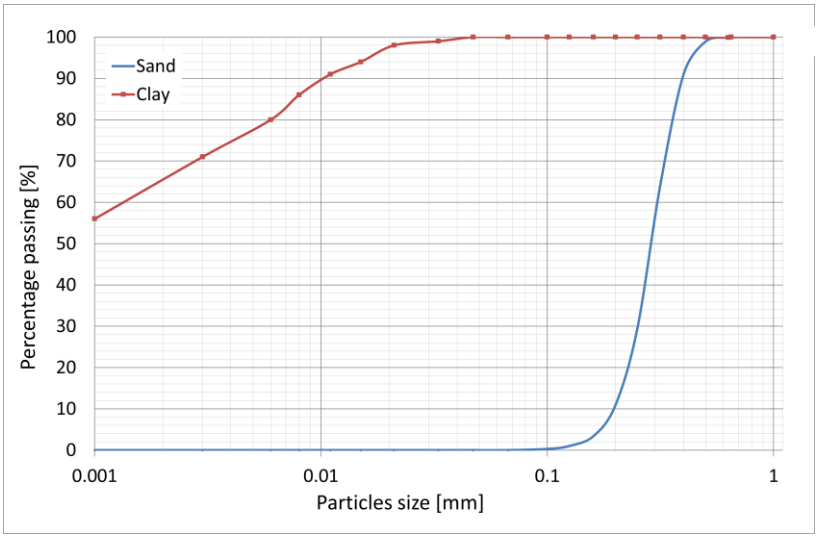

Fig 1. Particle size distribution of the components of this reconstituted soil.

Table 1. Chemical composition of kaolinite and sand.

Chemical element	SiO_2	Al_2O_3	Fe_2O_3	MgO	K_2O	Na_2O	TiO_2	CaO	I_2O_3
Kaolinite (%)	48 - 50	35 - 37	0.6 - 0.8	0.2 - 0.4	1.9 - 2.3	0.1 - 0.2	0.04 - 0.06	0.09 - 0.11	-
Sand (%)	> 99	-	0.02	-	0.5	-	0.025	0.01	0.95

Three different mixes of clay and sand were studied with two water content configurations: at the mixing moisture state and after stabilized drying at 50% of relative humidity and 20 °C. The first mix, composed of only clay (0S), was used to obtain the characteristics of the clayed matrix only. The second mix contained 30% of sand (30S) and the third 60% of sand (60S). Table 2 summarizes the composition of the three mixes. In these three mixes, the sand content is low enough to deem the clayed matrix as continuous (another assumption of homogenization theory).

Table 2. Composition of the three mixes analyzed.

Mixes	0S	30S	60S
Kaolinite (%)	100	70	40
Sand (%)	0	30	60
Mixing moisture content ω (%)	30	21	12

2.2 Procedures

2.2.1 Sample preparation

Depending on the test, two different sample shapes were used: a cylinder (height = 10 cm, diameter = 5 cm) for the compressive tests and the measurement of Young's modulus, and a prismatic sample (15 cm*15 cm*5 cm) for assessing thermal conductivity, shrinkage and tensile strength (Fig 2). First, sand and clay were mixed manually to create a homogenous mix. Then water was added and the whole material was mixed with a mixer. After putting the material in an airtight box for 24h to allow water diffusion in the smallest pores, both samples were created by compaction in a metallic mold (pressure = 1 MPa).

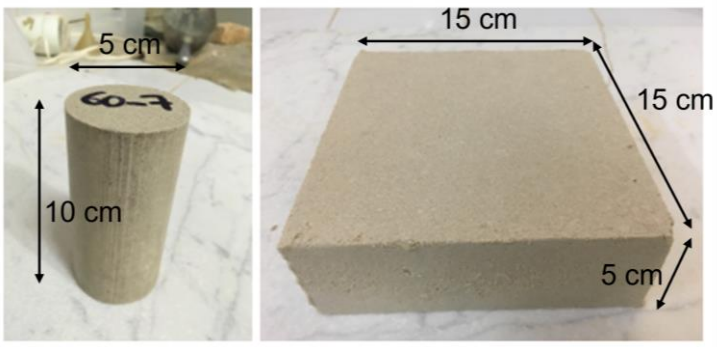

Fig 2.Cylindrical and prismatic samples used to determine the mechanical and thermal properties of this reconstituted soil.

To determine the required water content to manufacture the samples, a Proctor compaction test was carried out in accordance with the NF P94-093 standard [31]. We compared the ratio between water content and clay content that corresponded to the highest dry bulk density for the three mixes. As the ratio was close to 0.3 for all mixes, we decided to keep the ratio constant in order to obtain an identical clayed matrix, which was useful for comparing the model (see Table 2 for the water content of each mixes).

Once the samples were created, half of them were tested immediately (saturated samples) while the other half were left to dry in a climatic chamber with a controlled temperature of 20 °C and relative humidity of 50%. The samples were weighted every day to keep track of water loss. Once the mass variation was lower than 2% for more than three days, the samples were tested. Each of the tests was performed on three samples for each sand and water content.

2.2.2 Geotechnical and physical characterization

Several geotechnical and physical tests were conducted to characterize the three mixes. First, the Atterberg limits of the three reconstituted soils were determined in accordance with the NF EN ISO 17892-12 standard [32]. Then, the bulk density of each mix was determined by: (i) measuring the sample dimensions with a precision caliper and deducing the volume of the sample from these dimensions, and (ii) dividing the corresponding weight (for the two different sample shapes) by this volume. While the samples were built to be perfectly cylindrical and prismatic, this was not always the case. Consequently, we expected to obtain scattered results, especially for the prismatic samples, which had more defects than the cylindrical samples.

We measured material porosity using a mercury intrusion porosimeter on small pieces of cylindrical and prismatic samples, in accordance with the ISO 15901-1:2016 standard [33]. The pressure in the cell decreases until a vacuum is created, but dried samples are required to that end. For this reason, the material was dried at 105 °C before testing and measuring the porosity of saturated samples was not possible. After the vacuum has been reached, the pressure in the cell increases gradually up to 400 MPa.

The sorption isotherm was measured with a dynamic vapor sorption (DVS) analyzer. A small, dried fragment of a sample is placed on a weighing machine to measure weight loss as the relative humidity of the DVS progressively evolves. First, the relative humidity increases from 0% to 97% (in 10% steps) to determine the sorption curve. Then, the relative humidity decreases (also in 10% steps) to determine the desorption curve. As was the case with the porosity test, small fragments from the cylindrical and prismatic samples were dried at 105 °C before testing.

2.2.3 Mechanical properties

Compressive strength

Measurements of compressive strength in earth samples can be greatly affected by the shape of the sample and the interface between samples and press platens [34], [35]. Several studies have shown the differences between cylindrical and prismatic samples for compressed earth blocks and rammed earth [36], [37]. Maniatidis and Walker [37], for example, demonstrated that the compressive strength measured on a cylindrical sample of reconstituted earth was higher than the strength measured on the prismatic sample. The presence of angles in the mold reduces compaction efficiency during sample fabrication, thus reducing the strength. To limit the negative effect of the angles, the samples used for the compression test were cylindrical. Sample slenderness was adjusted to 2 to limit friction with press platens. As the material is heterogeneous, the samples should be five times larger than the largest grain size for the material to be considered as homogenous [38]. In this study, the sand was very fine, and the cylinders were 10 cm high and 5 cm in diameter.

The compression tests were performed with a hydraulic press. As there is no existing standard for testing this type of material, the NF EN 13286-53 standard [39], which concerns the fabrication of cylindrical samples for testing road material, was used for the fabrication of the samples, while the NF XP P 13-901 standard [29] for compression tests of compacted earth blocks was adapted to this case. As sample slenderness was equal to 2, there was no specific bracing system. The press was controlled by force, with its speed being set to 0.02 kN/s to limit the effect of velocity during the test.

Young's modulus E and Poisson's ratio ν

Young's modulus is calculated from the strain–stress relation. Strain measurement is difficult and can lead to scattered results. Mollion [40] compared the Young's modulus obtained when the strain is determined by the displacement of the press (global) and when it is determined by gauges placed at the center of the sample (local). The friction between the sample and the experimental setup induces a large difference between local and global Young's modulus. To determine the Young's modulus of a sample, the strain must be measured at a portion of the sample where friction phenomena is nonexistent. Moreover, Young's modulus should be measured with loading-unloading cycles. If these two criteria are not respected, the precision of the results will be lower e.g. in the study of Kouakou et al. [41], the displacement of the platen was measured without using loading-unloading cycles).

In this study, the strain–stress relation for each mix was determined with video correlation acquired during a compressive test with three unloading/loading cycles (Fig 3). During these cycles, the load progressively increased until 33% of the compressive strength was reached, subsequently decreasing until 10% of the compressive strength was reached. The hydraulic press was tested by force for the dried samples (speed = 0.02 kN/s) and by displacement for the saturated samples (speed = 0.5 mm/min). A different approach for saturated samples is necessary because of their low compressive strength, which is difficult to obtain with enough precision with a test

by force. A polytetrafluoroethylene plate has been used on the top and bottom of the sample to limit the friction between the material and the press. Using this approach, it was also possible to determine the radial strain of the sample and to deduce from it the Poisson's ratio of the material.

Young's modulus and Poisson's ratio were determined with the slope of the strain–stress relation during the cycles, while tangent moduli E_t were determined with the slope of the strain–stress relation before the beginning of the cycles.

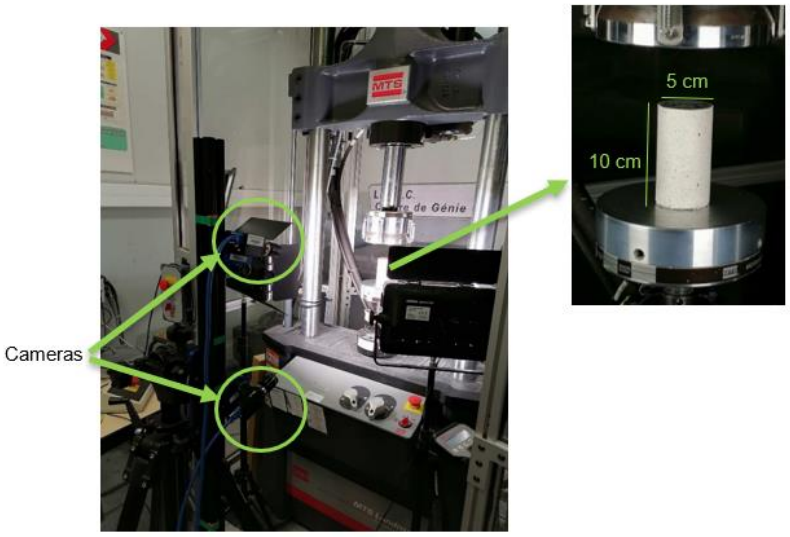

Fig 3. Video correlation set-up

Tensile strength

While there is no existing standard for measuring tensile strength, three-point bending tests and Brazilian tests are often used in the literature [38]. We opted for a three-point bending test, using the same hydraulic press employed in the compressive test. The press was controlled by force with a speed of 0.02 kN/s. The samples were prismatic blocks (15 cm*5 cm*5 cm) obtained by cutting the rectangular samples (Fig 2) in three parts with a diamond saw. The two lower contact points were placed at 1 cm from the border of the samples (Fig 4).

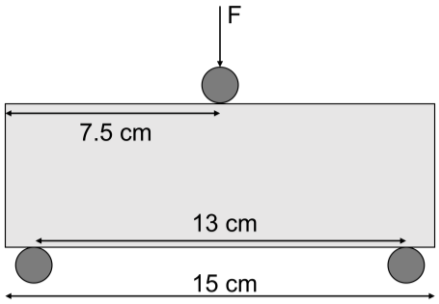

Fig 4. Boundary conditions of the three-point bending test.

Shrinkage

The standard commonly used to determine earth shrinkage, NF P 94-060 [42], requires a material with a water content close to the liquid limit of the soil. This standard was not relevant for the present study since the main objective was to produce cohesive samples allowing the determination of all studied properties with the same clayed matrix (with the same fabrication method for all the mixes). The water content of the three mixes was thus closer to the plastic limit than to the liquid limit. A new and simple measurement device is proposed to measure linear shrinkage in one direction (Fig 5).

A 15 cm*15 cm*5 cm prismatic sample was manufactured by compaction, using a similar approach than the compression test. The shape of the sample was chosen so that a thermal conductivity test could be carried out after drying. The measurement device designed for this specific study consisted of three fixed borders and a moving one. All the borders, including the bottom of the device and the moving border, were covered with polytetrafluoroethylene to ensure that no friction would occur between the sample and the fixed and moving parts of the structure. As illustrated in Fig 5, the sample was smaller than the box to easily place the sample inside. Once it was centered, the moving border was put in contact with the sample with two mechanical displacement sensors maintaining this position. The sensors applied a small force through their springs in the middle of the sample (height-wise). These mechanical sensors can measure a displacement with a precision of 0.005 mm. The measurement

device was set up on a weighing machine to simultaneously measure displacement and weight loss without needing to move the device. The whole system was conserved in a climatic chamber at 50% of relative humidity and 20 °C. Once the displacement and weight variation between two consecutive days was lower than 2%, the measurement was terminated.

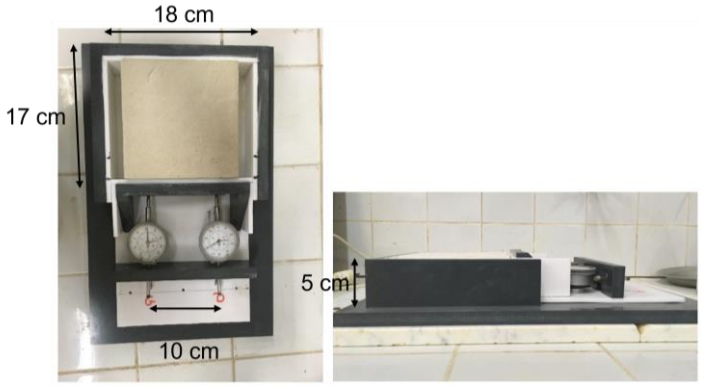

Fig 5. Shrinkage measurement device.

2.2.4 Thermal properties

Thermal conductivity

There are two different methods to determine the thermal conductivity of a material, which can lead to different results: the guarded hot plate and the hot-wire method [38]. Here, we measured thermal conductivity with the guarded hot plate method in accordance with the NF EN 12667 standard [43]. Prismatic samples were prepared with earth compaction to respect the dimensions recommended by the standard. Since dried and saturated tests were made for each composition, it was necessary to take water loss into consideration during the test. To limit water loss, all the samples were wrapped in cling film. A variation of mass lower than 1% was noticed during the test. The temperature of the hot plate was set to 25 °C and the temperature of the cold plate was set to 15 °C. The measurement was terminated when the variation of conductivity was lower than 1% for 90 min.

Specific heat capacity

Specific heat capacity can be measured by means of differential scanning calorimetry (DSC). The NF EN ISO 11357 standard [44] was used to determine the specific heat capacity of each mix. The material was used in its powder form. The particles were manually ground with an agate mortar until they were smaller than 40 µm and dried in an oven at 40 °C for one week. The specific heat capacity of the saturated mixes was determined from the specific heat capacities of the dried mix and water at 20 °C, according to the following expression [23]:

$$c(w) = c_{dry} + w \cdot c_{water} \qquad (2.1)$$

With $c(\omega)$ the specific heat capacity of a material containing water, c_{dry} the specific heat capacity of the same material dried and $c_{water} = 4.181\ J/(g.K)$ the specific heat capacity of water.

3 RESULTS AND DISCUSSION

3.1 Geotechnical and physical characterization

3.1.1 Atterberg limits and Proctor tests

The Atterberg limits of the three reconstituted soils and the corresponding standard deviations are presented in Table 3. Regarding the liquid limit (ω_L), we noticed that the ratio of water content (ω) to clay content (cl) was notably similar for all the mixes. This assertion also holds true for the plastic limit (ω_P). Liu and Tong [14] analyzed soils with different kaolinite clay contents and obtained slightly different results. This difference might result from the presence of silt in their soils, which can influence material consistency. This could imply that the fine particles, which constitute the clayed matrix in this study, are responsible for material consistency and that the presence of sand has no impact on it. In this table, the plasticity index I_p, which is the difference between liquid and plastic limits, is given.

Table 3. Atterberg limits of the three mixes (0S, 30S and 60S).

	0S	30S	60S
ω (%)	30	21	12
ω_L (%)	64.6 ± 3.9	43.2 ± 1.5	25.7 ± 1.4
ω_L/cl	0.65	0.62	0.64
ω_P (%)	35.4 ± 3.0	23.8 ± 2.1	15.6 ± 1.1
ω_P/cl	0.35	0.34	0.39
I_P (%)	29.2 ± 4.9	19.4 ± 2.9	10.2 ± 2.5

The results obtained from the Proctor tests are given in Fig 6 and Table 4. The maximal dry bulk density was obtained when the water content (ω) was close to the plastic limit of the mix, which is consistent with the observations from other studies that used the plastic limit as the fabrication water content [15], [41], [45].

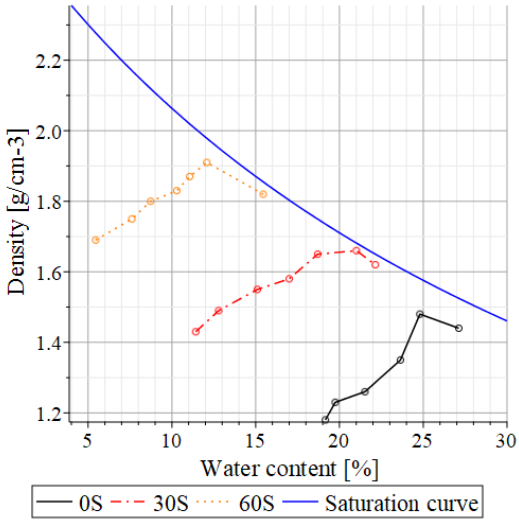

Fig 6. Proctor curves of the three mixes (0S, 30S and 60S).

Table 4. Dry bulk densities obtained with Proctor compaction tests.

	0S	30S	60S
$\gamma_{dProctor}$ $(g.cm^{-3})$	1.48	1.66	1.91
$\omega_{Proctor}$ (%)	25.4	21.0	12.1

3.1.2 Physical characterization

The dry bulk density γ_d, the saturated bulk density γ_{sat}, the real density γ_s and the porosity n of each mix are presented in Table 5. The average values and standard deviations obtained from the cylindrical and prismatic samples were similar. For this reason, Table 5 only presents the results from the cylindrical samples. It was not possible to obtain samples from the corner of the bricks to determine whether it exists defects resulted from the shape of the mold. As expected, the density of the samples increases with the sand content. The porosity increased linearly with the clay content of the mix. Moreover, the pore sizes observed with the porosimeter (Fig 7a) are approximately 100 nm, which is the same magnitude as clay. These two elements might indicate that the porosity is mostly located in the clayed matrix (clay and water). Previous studies have measured the porosity of raw earth bricks with mercury intrusion porosimetry [46]–[48], obtaining porosity values between 21 and 35%. The pore size distribution of these measurements is not similar for all the soils, with the pore size varying between 100 nm and 10 µm.

Table 5. Physical characteristics of the samples.

	0S	30S	60S
γ_{sat} $(g.cm^{-3})$	1.80 ± 0.01	1.96 ± 0.01	2.14 ± 0.01
γ_d $(g.cm^{-3})$	1.50 ± 0.02	1.72 ± 0.03	1.92 ± 0.01
γ_s $(g.cm^{-3})$	2.6	2.6	2.6
n(%)	43.7 ± 0.7	36.6 ± 0.9	30.6 ± 0.9

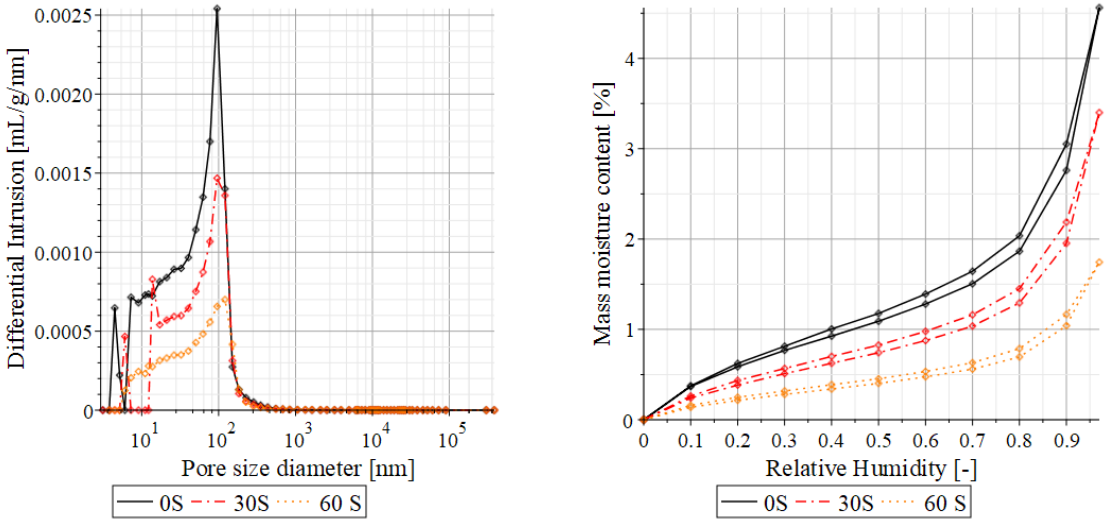

(a) *(b)*

Fig 7. Pore size diameter (a) and sorption isotherms (b) of each mix (0S, 30S and 60S).

Fig 7b illustrates the sorption and desorption curves of the three mixes. The hysteresis phenomenon between the sorption and desorption curves is low. This behavior might be explained by the tight pore size distribution (Fig 7a), which highlights a good connection between the pores. Moreover, the maximal moisture content is higher for the mix containing more clay, indicating that the clay is able to interact and absorb more water than the sand. Some authors have measured the sorption and desorption curves of earth bricks [4], [46], [49], where the maximal mass moisture content of their soils ranged between 3 and 6%. The results of this study were not different (Fig 7b) except for the mix containing 60% of sand, which is lower. As previously evidenced by McGregor et al. [4], the difference in maximal moisture content between two soils can also be explained by the type of clay, which greatly affects water absorption on earthen materials. With an expansive clay, such as smectite, the water absorption of earthen material will be more important than with a non-expansive clay, such as kaolinite used in this study.

3.2 Mechanical properties

3.2.1 Compressive strength R_c

The mechanical properties measured in this experimental campaign and their standard deviation are summarized in Table 6. As shown in Fig 8a, the compressive strength (R_c) of the dried and saturated samples linearly increased with the sand content and the density of the samples. This evolution can be explained by the presence of sand in the material which increases the resistance of the material. Moreover, it was observed that the strength of the material was higher for dried samples than for wet ones. The standard deviation was low, indicating that the fabrication protocol did not significantly affect the compressive strength of the material.

Table 6. Mechanical properties.

			0S	30S	60S
Saturated	Rc	MPa	0.11 ± 0.02	0.22 ± 0.01	0.33 ± 0.02
	Rt	MPa	0.052 ± 0.003	0.060 ± 0.003	0.121 ± 0.022
	E	MPa	35 ± 18	20 ± 8	18 ± 3
	E_t	MPa	19.4 ± 8	3.5 ± 1.8	1.6 ± 0.2
	ν	-	0.24 ± 0.01	0.39 ± 0.12	0.46 ± 0.01
Dried	Rc	MPa	0.99 ± 0.18	1.16 ± 0.13	1.28 ± 0.10
	Rt	MPa	0.40 ± 0.06	0.37 ± 0.08	0.23 ± 0.02
	E	MPa	262 ± 32	832 ± 100	1191 ± 69
	E_t	MPa	108 ± 42	784 ± 331	938 ± 299
	ν	-	0.30 ± 0.02	0.34 ± 0.04	0.40 ± 0.02
	ε_r	%	3.66 ± 0.21	2.68 ± 0.23	0.76 ± 0.11
	Δm	%	24.19 ± 0.41	18.26 ± 0.22	11.1 ± 0.24

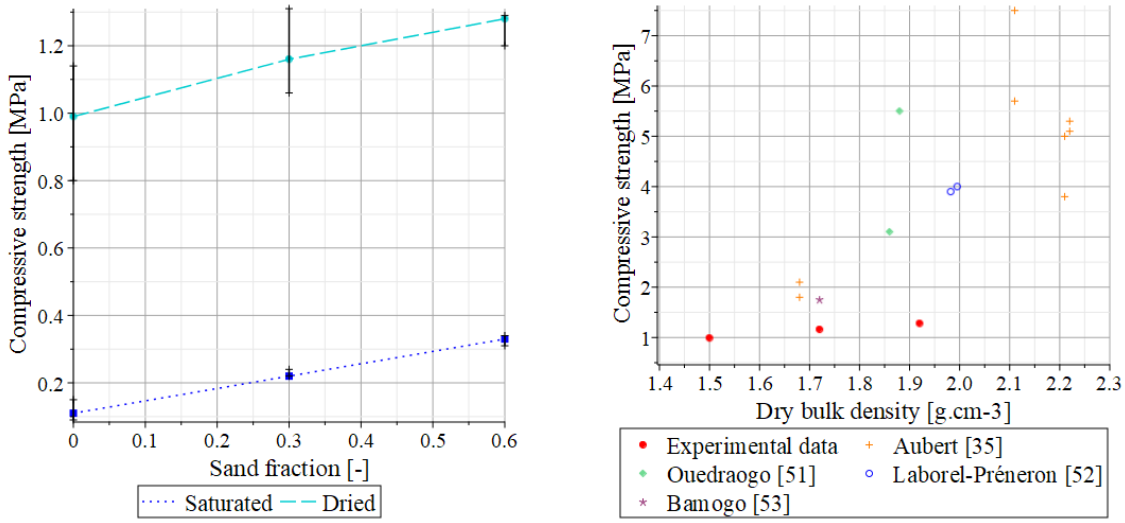

(a) (b)

Fig 8. Evolution of the compressive strength of the samples as a function of sand content (a); experimental data (from the dried samples) and literature review comparison of compressive strength as a function of dry bulk density (b).

Numerous studies [12], [41], [45], [50] have shown that the compressive strength increases with the density in soils with similar components. Fig 8b illustrates the relation between compressive strength and dry bulk density for different types of soil, comparing the experimental data of this study with data from four other studies. Ouedraogo et al. [51] and Laborel-Prérenon et al. [52] chose the same method of fabrication as us but using samples 5 cm high, while Bamogo et al. [53] and Aubert et al. [35] used compressed bricks of various dimensions. We observed that the results vary significantly for similar densities. The compressive strength values obtained in this study are lower than those obtained by others, which could be explained by the composition of the samples (pure kaolinite and the uniform grain size distribution of the sand).

The compressive strength varied significantly with the moisture content (Table 6). The presence of water in the pores induces capillary pressure (or suction), enhancing the cohesion of the material. The lower the water content, the smaller the pores filled with water and the higher the capillary pressure. If the water content is too high, the suction will not be strong enough to ensure cohesion and the compressive strength will decrease. Bui et al. [22] and Laou et al. [46] studied the effect of water content and suction on the compressive strength. Their results highlighted a strong correlation between strength and suction.

3.2.2 Young's modulus E and Poisson's ratio ν

Many studies have measured Young's modulus E during compressive tests [14]–[17], [19], with the results showing significant dispersion (30–1000 MPa) [13]. The dispersion can be explained by the variability of earth compositions, the moisture content and the shape and size of the samples. Alternatively, the heterogeneity of the results can result from the lack of a standard to measure the Young's modulus on raw earth. Consequently, the measuring protocols can vary significantly from one study to another. The first difference concerns the loading path, with some authors opting for a simple compressive test [16], [17], [46], [54] to measure the modulus and others opting for a cyclic compressive test [54]. The second difference lies in the strain measurement approach: in some studies, a strain gauge was employed directly on the samples [54], while in others the displacement of the platen of the press was measured [16], [17], [46]. Champire et al. [54] measured the Young's modulus of three different earths using video correlation, obtaining values ranging from 1 to 5 GPa. In this experimental study, the order of magnitude of the Young's modulus was ranging from 0.3 GPa to 1.2 GPa (Table 6) for dried samples, which was smaller than their results. However, the general behavior of the material was similar. Fig 9 illustrates the evolution of the axial and radial strains in a saturated sample containing 60% of sand as a function of the stress. The high values of the axial and radial strains highlight the significant deformation of the saturated samples during the test.

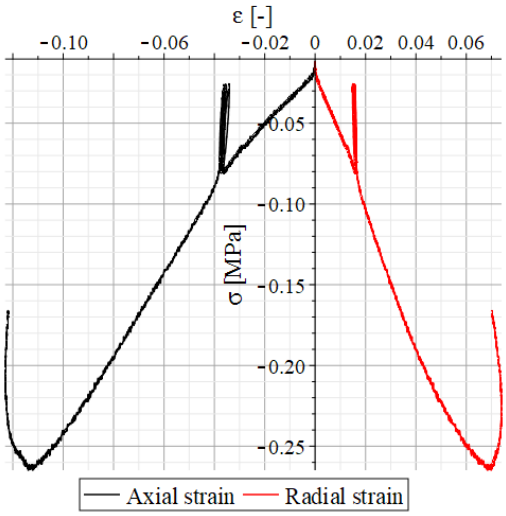

Fig 9. Evolution of the axial and radial strains (60S saturated sample) as a function of the stress.

The relevance of the water content on the properties of the material can be observed in Table 6 and Fig 10a. A significant difference between dried and saturated samples can be noticed. The values of the Young's modulus of wet samples are so low that analyzing the differences between the three mixes does not seem relevant, while a comparison is possible for the dried samples. As ~~for~~ in the compressive strength, the Young's modulus increases with the sand content.

The Poisson's ratio is ranging from 0.25 to 0.45 (Table 6). In Fig 10b, it is observed that the Poisson's ratio increases as a function of clay content, but the water does not seem to impact in a specific way this property. Few authors have measured Poisson's ratio ν, with results in the literature ranging from 0.15 to 0.45 [11], [19], [21]. The results of this study are thus consistent with these observations.

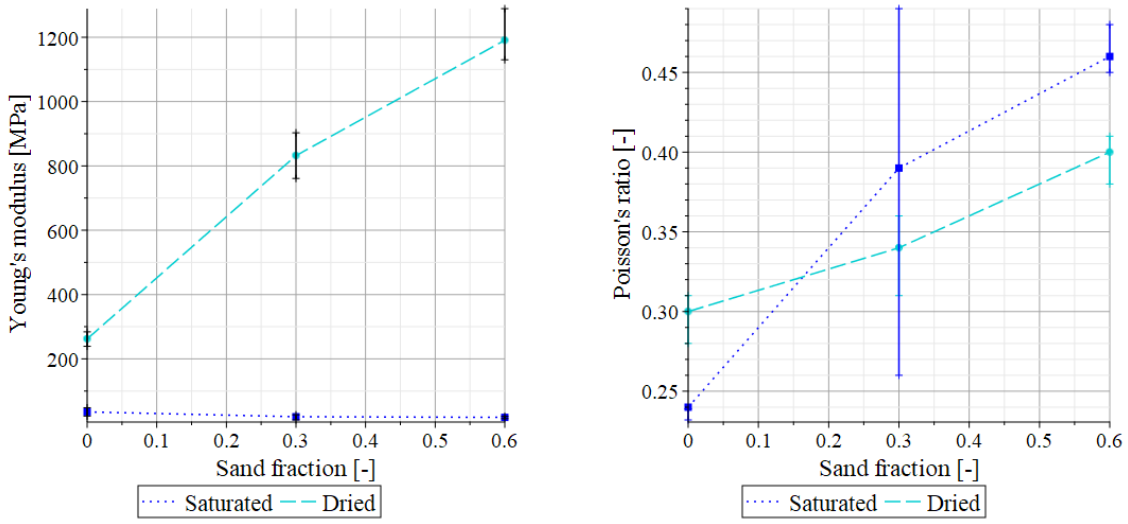

(a) *(b)*

Fig 10. Evolution of Young's modulus (a) and Poisson's ratio (b) of the samples as a function of sand content.

3.2.3 Tensile strength R_t

The tensile strength (R_t) of earth is difficult to measure directly, which explains the scarcity of experimental results in the literature. However, some authors have determined the tensile strength of earth materials using Brazilian tests [11], [16], [19], [20], [55], [56]. The values obtained are all lower than 0.52 MPa [11] and the ratio between the tensile and compressive strengths varies between 0.1 and 0.2. In this study, the ratio ranged between 0.2 and 0.5, depending on the water content of the sample. This large difference might highlight the necessity to experimentally determine the tensile strength of earth, since it cannot be easily linked to the compressive strength.

The results summarized in Table 6 and illustrated in Fig 11 indicate a low tensile strength. In the dried samples, the strength decreased as the sand content increased; the opposite phenomenon was observed in the saturated samples. It is clear that the sand content reduces the cohesion of the material.

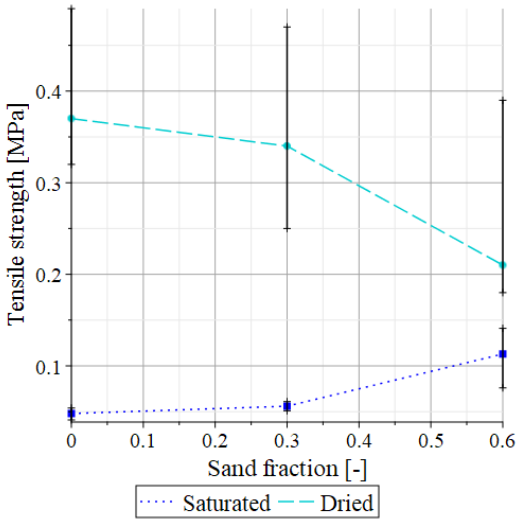

Fig 11. Evolution of the tensile strength of the samples as a function of sand content.

3.2.4 Shrinkage ϵ_r and mass loss Δm

Fig 12 shows the shrinkage behavior of the three mixes as a function of water content. For the sake of comparison, the relative water content, defined as the ratio of water content to the initial water content, was used. In the graph, shrinkage is defined as the relative length of the sample, which corresponds to the ratio of length variation in the measured direction to the initial length. It is worth noting that the shape of these curves is similar to the clay shrinkage curve defined by Chertkov [57] and is consistent with the results obtained by Bahar et al. [45]. The shrinkage is linear until it reaches a plateau, with the end of the linear portion of the curve corresponding to the air entering the pores. The curves also indicate that the samples continue losing water when the shrinkage is over. In Fig 12, the mix containing the highest content of clay presents the highest shrinkage. This phenomenon can be explained by the fact that the presence of sand grains inside the clay limits the possible shrinkage.

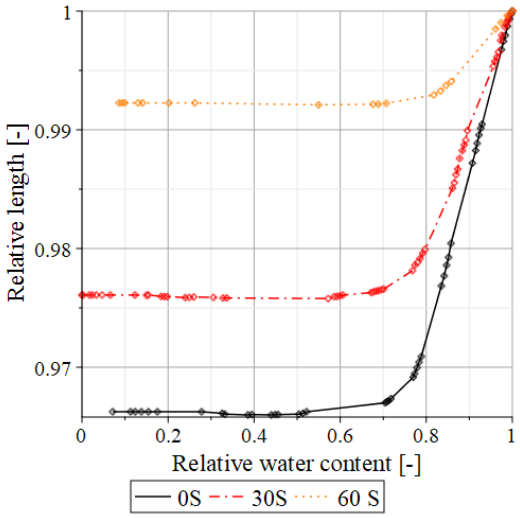

Fig 12. Shrinkage curves for the three mixes (0S, 30S and 60S).

Final linear shrinkage values and their associated standard deviation are reported in Table 6. The shrinkage increased as the sand content decreased, as observed in [45] and [58]. The order of the magnitude of the observed shrinkage is consistent with other values found in the literature (Table 7). However, considering the high number of the parameters affecting earth shrinkage, such as the molding water content, the clay content, the type of clay and the particle size distribution of the sand, it is difficult to compare the results obtained from different studies (which analyze different soils with various methodologies) without a model that takes into account all these parameters.

Table 7. Linear shrinkage values found in the literature.

Ref.	Type of clay	cl (%)	ω (%)	ϵ_r (%)
Present study	kaolinite	40–100	12–30	0.76–3.66
Heath et al. [59]	nd	25–38.1	nd	7–10
Walker et al. [58]	kaolinite	20–90	nd	0.4–12.8
Bouhicha et al. [60]	nd	21–40	19–28	4–8
Sangma et al. [61]	nd	14.25	31.7–40	3.18–5.21

3.3 Thermal properties

The thermal conductivities (λ) and specific heat capacities (c) for the three soil compositions and their standard deviation are presented in Table 8. Thermal conductivity measurements were not scattered between the three tests series, indicating that sample fabrication does not have an impact on thermal conductivity; this parameter was mainly affected by the composition of the material.

Table 8. Thermal properties.

			0S	30S	60S
Saturated	γ_{sat}	g/cm^3	1.80 ± 0.01	1.96 ± 0.01	2.14 ± 0.01
	λ	W/(m.K)	1.15 ± 0.08	1.34 ± 0.06	1.00 ± 0.09
	c	J/(g.K)	2.04 ± 0.10	1.84 ± 0.19	1.29 ± 0.01
Dried	γ_d	g/cm^3	1.50 ± 0.02	1.72 ± 0.03	1.92 ± 0.01
	λ	W/(m.K)	0.40 ± 0.01	0.54 ± 0.02	0.70 ± 0.08
	c	J/(g.K)	1.01 ± 0.14	1.14 ± 0.25	0.88 ± 0.01

Many authors have measured the thermal conductivity of earth in different forms, adobe [7], [62], [63], rammed earth [23], [24], [64], [65], cob [66], and with different measurement devices, transient-state measurements with hot wire [62], [63], [66] or surface probes [23], [65] and steady-state measurements with a guarded hot plate [7], [24], [49], [51], [64]). Fig 13 illustrates thermal conductivity as a function of dry bulk density measured in some of these studies using a guarded hot plate (for samples with low water content). The results from this experimental campaign (for dried samples) are plotted in the same figure, showing that their magnitude is consistent with the literature with the guarded hot plate. The thermal conductivity of dried samples seems to increase with the dry bulk density. Moreover, the dried bulk density seems to be linked to the porosity (Table 5) of the material: the more porous a material is, the lower its thermal conductivity. Laurent [23] noted a similar results with the 10 different rammed earth he has analyzed.

Table 8 also describes the evolution of thermal conductivity as a function of water content. The thermal conductivity is higher when the degree of saturation is higher, but the pattern seems to be different for all the analyzed mixes. Hall and Allinson [24] showed that thermal conductivity increases linearly with the degree of saturation of a sample, with the slope of the linear relationship varying with the density of the sample. This linear evolution cannot be confirmed by these results because only two degrees of saturation have been tested. However, it can be noticed that the increase of the thermal conductivity between the dried samples and the corresponding saturated samples is lower for the samples without sand than for the samples containing 30% of sand. This confirms the statement of [24]. However, the conductivity of some sands may be lower than that of water [67]. Therefore, the addition of a large amount of sand can theoretically decrease the thermal conductivity of some mixtures, which could explain the behavior observed of saturated samples.

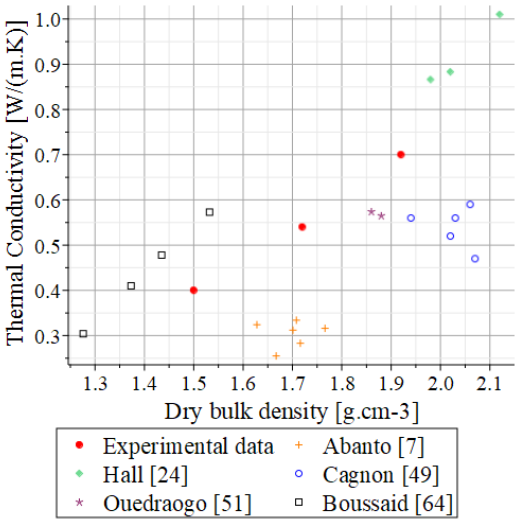

Fig 13. Thermal conductivity of earth samples measured with a guarded hot plate.

Several authors have measured the specific heat capacity of earth, finding values that range between 0.800 and 1.200 J/(g.K) [5], [8], [23], [49], [62], [66], [68]. The values obtained in this study (Table 8) are consistent with these measurements. The evolution of the specific heat capacity of the dried samples does not seem to follow a notable evolution as a function of the sand content. For saturated samples, the specific heat capacity values depend on the water contents of fabrication, which was to expect as they were determined from the results of the dried samples and Equation (2.1).

3.4 Discussion

The results confirm the negative impact of increasing sand and water contents on the thermal conductivity. However, they increase the thermal inertia which confirms the interest of earth material for the design of eco environmental constructions.

Concerning the mechanical properties of dried samples, when sand content increases, compressive strength and Young's modulus tend to increase and shrinkage decreases. Thus, these properties are improved as expected. However, simultaneously, the tensile strength decreases which means that this material performance is lower. Even if the presence of sand seems to benefit to the compressive strength, the Young's modulus and the shrinkage, it reduces significantly the tensile strength. The reason could be related to the balance between shrinkage reduction and tensile strength reduction which affects the mechanisms of cracking of earthen materials. During the drying, the sand restrains the clay shrinkage resulting in a stress concentration around aggregates, so the benefit of capillary pressure on local tensile strength of the matrix is partially removed at the macro scale by this micro mechanism inducing crack initiation around aggregates.

4 CONCLUSION

This study deals with the characterization of three reconstituted soils containing kaolinite and fine sand in different proportions. The mechanical and thermal properties of the material, with two different moisture contents, were determined to assess the coupling effects of sand and water on the performance of earth construction materials.

Regarding the thermal properties of the material, the measurements of its thermal conductivity and specific heat capacity confirm previously published data for dried samples. Earth cannot be deemed a good insulating material solely on the basis of its thermal conductivity, which is ranging from 0.4 W/(m.K) without sand to 0.7 W/(m.K) with 60% of sand. The ability of earth to provide thermal comfort is possible because of its thermal inertia, which is positively affected by the increase of density and specific heat capacity.

The mechanical characterization highlighted how the composition of earth, and especially the sand and water content, affects the properties of the material. First, for dried samples (RH 50%), as the sand content increases from 0 to 60%, the compressive strength increases from 0.99 to 1.28 MPa, the Young's modulus increases from 0.3 to 1.2 GPa and the tensile strength decreases from 0.4 to 0.23 MPa, showing the negative impact of sand on tensile strength during drying. Secondly, the water inside the material interacts with the clay, also affecting the compressive strength and tensile strength. For example, for the mix containing 30% of sand, the compressive (respectively tensile) strength varies from 0.22 (respectively 0.06) MPa at the fabrication water content to 1.16 (respectively 0.37) MPa after drying at 50% RH. These observations are consistent with data found in the literature.

A new measurement device was developed to measure earth shrinkage on a sample with the same fabrication water content as the samples used for other tests. The device measures the unidirectional shrinkage of a brick with two mechanical sensors. The final shrinkage values, ranging from 3.66% without sand to 0.76% with 60% of sand, are consistent with the data obtained in the literature (on earth samples containing mostly kaolinite). It should be noted that shrinkage is largely affected by the type of clay present in the material and that results can vary significantly from one earth composition to another. The capillary pressure of the micropores increases when the material dries and enhances the cohesion of the material. However, the sand by limiting the shrinkage may produce

stress concentrations in the vicinity of aggregates leading to damages in the clayed matrix which reduces the apparent tensile strength of the mix.

Since the earth composition was entirely known in this experimental design, the variability of the material was solely a result of the fabrication process. We chose a specific composition (clay and sand) to facilitate using the experimental results in a model based on homogenization procedures. Such a model could be used to predict the performance of a material depending on its composition. However, seeing as earth is composed of many different types of clay and sand in various proportions, this experimental campaign is not sufficient to predict the behavior of all earth types. Undertaking a campaign with other types of clay, sand and water contents would complement the experimental data obtained in this study. The standard deviation was quite low throughout the study, indicating that variability is limited when the composition of the material is well known. In a next stage, we will seek to develop a homogenization model able to predict the variability of the properties of a material depending on the variability of its composition. Such a prediction would be useful to define the earth composition variability for which the properties of the material are suitable for construction.

5 REFERENCES

[1] Commissariat Général au développement durable, “Chiffres clé de l’énergie,” 2014.

[2] G. Minke, *Building with earth : Design and Technology of a Sustainable Architecture*. Berlin, 2009.

[3] A. Fabbri, N. Al Haffar, and F. McGregor, “Measurement of the relative air permeability of compacted earth in the hygroscopic regime of saturation,” *Comptes Rendus Mec.*, vol. 347, pp. 912–919, 2019.

[4] F. McGregor, A. Heath, A. Shea, and M. Lawrence, “The moisture buffering capacity of unfired clay masonry,” *Build. Environ.*, 2014.

[5] D. Allinson and M. Hall, “Hygrothermal analysis of a stabilised rammed earth test building in the UK,” *Energy Build.*, no. 42, pp. 845–852, 2010.

[6] T. Morton, F. Stevenson, B. Taylor, and N. C. Smith, “Low cost earth brick construction : 2 Kirk Park, Dalguise : monitoring & evaluation,” [Communities Scotland], 2005.

[7] G. A. Abanto, M. Karkri, G. Lefebvre, M. Horn, J. L. Solis, and M. M. Gomez, “Thermal properties of adobe employed in Peruvian rural areas: Experimental results and numerical simulation of a traditional bio-composite material,” *Case Stud. Constrution Mater.*, vol. 6, pp. 177–191, 2017.

[8] M. Hall and D. Allinson, “Analysis of the hygrothermal functional properties of stabilised rammed earth materials,” *Build. Environ.*, vol. 44, pp. 1935–1942, 2009.

[9] J. Jeannet and G. Pollet, “La thermique du pisé,” in *Modernité de la construction en terre*, Plan Const., Paris, 1984.

[10] H. Houben and H. Guillaud, *Earth Construction : A Comprehensive Guide (Earth Construction)*, Intermedia. London, 1994.

[11] L. Miccoli, U. Muller, and P. Fontana, “Mechanical behaviour of earthen materials: A comparison between earth block masonry, rammed earth and cob,” *Constr. Build. Mater.*, vol. 61, pp. 327–339, 2014.

[12] J. C. Morel, A. Pkla, and P. Walker, “Compressive strength testing of compressed earth blocks,” *Constr. Build. Mater.*, vol. 21, pp. 303–309, 2007.

[13] F. Avila, E. Puertas, and R. Gallego, “Characterization of the mechanical and physical properties of unstabilized rammed earth: A review,” *Constr. Build. Mater.*, vol. 270, 2021.

[14] Q. Liu and L. Tong, “Engineering Properties of Unstabilized Rammed Earth with Different Clay Contents,” *J. Wuhan Univ. Technol.*, vol. 32, no. 4, pp. 914–920, 2017.

[15] V. Maniatidis and P. Walker, “Structural capacity of rammed earth in compression,” *J. Mater. Civ. Eng.*, vol. 20, no. 3, pp. 230–238, 2008.

[16] V. Toufigh and E. Kianfar, “The effects of stabilizers on the thermal and the mechanical properties of rammed earth at various humidities and their environmental impacts,” *Constr. Build. Mater.*, vol. 200, pp. 616–629, 2019.

[17] M. Kosarimovahhed and V. Toufigh, “Sustainable usage of waste materials as stabilizer in rammed earth structures,” *J. Clean. Prod.*, vol. 277, 2020.

[18] F. Champire, “Étude expérimentale du comportement hydro-mécanique de la terre crue compactée pour la construction,” Université de Lyon, 2017.

[19] T.-T. Bui, Q. B. Bui, A. Liman, and S. Maximilien, “Failure of rammed earth walls: From observations to quantifications,” *Constr. Build. Mater.*, vol. 51, pp. 295–302, 2014.

[20] Q. B. Bui, T.-T. Bui, R. El Nabouche, and D.-K. Thai, “Vertical Rods as a Seismic Reinforcement Technique for Rammed Earth Walls: An Assessment,” *Adv. Civ. Eng.*, 2019.

[21] R. El Nabouche, “Mechanical behavior of rammed earth walls under Pushover tests,” Université de Grenoble, 2017.

[22] Q. B. Bui, J. C. Morel, S. Hans, and P. Walker, “Effect of moisture content on the mechanical characteristics of rammed earth,” *Constr. Build. Mater.*, vol. 54, pp. 163–169, 2014.

[23] J.-P. Laurent, “Propriétés thermiques du matériau terre,” *Cah. du CSTB*, vol. 279, p. 2156, 1987.

[24] M. Hall and D. Allinson, “Assessing the effects of soil grading on the moisture content-dependent thermal conductivity of stabilised rammedearth materials,” *Appl. Therm. Eng.*, no. 29, pp. 740–747, 2009.

[25] A. Fabbri, J. C. Morel, J. E. Aubert, Q. B. Bui, D. Gallipoli, and B. . Reddy, *Testing and Characterisation of Earth-based Building Materials and Elements*. Springer, Cham, 2022.

[26] R. Anger, “Approche granulaire et colloïdale du matériau terre pour la construction,” 2011.

[27] A. Meunier, *Argiles*, Editions S. 2002.

[28] NF EN ISO 17892-4, “Reconnaissance et essais géotechniques - Essais de laboratoire sur les sols - Partie 4 : Détermination de la distribution granulométrie des particules,” 2018.

[29] XP P13-901, “Blocs de terre comprimée pour murs et cloisons. Définition - Spécifications - Méthodes d’essai - Conditions de réception,” 2001.
[30] NF EN 1097-6, “Essais pour déterminer les caractéristiques mécaniques et physiques des granulats - Partie 6 : Détermination de la masse volumique réelle et du coefficient d’absorption de l’eau,” 2014.
[31] NF P94-093, “Sols : reconnaissance et essais - Détermination des références de compactage d’un matériau - Essai Proctor Normal - Essai Proctor modifié,” 2014.
[32] NF EN ISO 17892-12, “Reconnaissance et essais géotechniques - Essais de laboratoire sur les sols - Partie 12 : Détermination des limites de liquidité et de plasticité,” 2018.
[33] ISO 15901-1:2016, “Evaluation de la distribution de taille des pores et la porosité des matériaux solides par porosimétrie à mercure et l’adsorption des gaz - Partie 1 : Porosimétrie à mercure,” 2016.
[34] J. E. Aubert, A. Fabbri, J. C. Morel, and P. Maillard, “An earth block with a compressive strength higher than 45 MPa!,” *Constr. Build. Mater.*, vol. 47, pp. 366–369, 2013.
[35] J. E. Aubert, P. Maillard, J. C. Morel, and M. Al Rafii, “Towards a simple compressive strength test for earth bricks?,” *Mater. Struct. Constr.*, vol. 49, no. 5, pp. 1641–1654, 2016.
[36] D. Ciancio and J. Gibbings, “Experimental investigation on the compressive strength of cored and molded cement-stabilized rammed earth samples,” *Constr. Build. Mater.*, vol. 28, no. 1, pp. 294–304, 2012.
[37] V. Maniatidis and P. J. Walker, “Structural capacity of rammed earth in compression,” *J. Mater. Civ. Eng.*, vol. 20, no. 3, pp. 230–238, 2008.
[38] M. Moevus, L. Fontaine, and R. Anger, “Caractéristiques mécaniques, thermiques et hygrométriques du matériau terre crue : bilan de la littérature,” Grenoble, 2012.
[39] NF EN 13286-53, “Mélanges traités et mélanges non traités aux liants hydrauliques - Partie 53 : méthode de confection par compression axiale des éprouvettes de matériaux traités aux liants hydrauliques,” 2005.
[40] V. Mollion, “Etude du comportement mécanique du pisé,” Lyon, 2009.
[41] C. H. Kouakou and J. C. Morel, “Strength and elasto-plastic properties of non-industrial bilding materials manufactured with clay as a natural binder,” *Appl. Clay Sci.*, vol. 44, pp. 27–34, 2009.
[42] XP P94-060-2, “Sols : reconnaissance et essais - Essai de dessication - Partie 2 : détermination effective de la limite de retrait sur un prélèvement non remanié,” 1997.
[43] NF EN 12667, “Performance thermique des matériaux et produits pour le bâtiment - détermination de la résistance thermique par la méthode de la plaque chaude gardée et la méthode fluxmétrique - Produits de haute et moyenne résistance thermique.”
[44] NF EN ISO 11357-1, “Plastiques - Analyse calorimétrique différentielle (DSC) - PArtie 1 : Principes généraux,” 2016.
[45] R. Bahar, M. Benazzoug, and S. Kenai, “Performance of compacted cement-stabilised soil,” *Cem. Concr. Compos.*, vol. 26, pp. 811–820, 2004.
[46] L. Laou, J. E. Aubert, S. Yotte, P. Maillard, and L. Ulmet, “Hygroscopic and mechanical behaviour of earth bricks,” *Mater. Struct.*, vol. 54, no. 3, pp. 1–15, 2021.
[47] F. Fouchal, F. Gouny, P. Maillard, L. Ulmet, and S. Rossignol, “Experimental evaluation of hydric performances of masonry walls made of earth bricks, geopolymer and wooden frame,” *Build. Environ.*, vol. 87, pp. 234–243, 2015.
[48] B. Remki, K. Abahri, R. Belarbi, and M. Bensaibi, “Hydric and structural approaches for earth based materials characterization,” *Energy Procedia*, vol. 139, pp. 417–423, 2017.
[49] H. Cagnon, J. Aubert, M. Coutand, and C. Magniont, “Hygrothermal properties of earth bricks,” *Energy Build.*, vol. 80, pp. 208–217, 2014.
[50] M. Olivier, “Le matériau terre, compactage, comportement, application aux structures en bloc sur terre,” INSA Lyon, 1994.
[51] K. A. J. Ouedraogo, J. Aubert, C. Tribout, and G. Escadeillas, “Is stabilization of earth bricks using low cement or lime contents relevant?,” *Constr. Build. Mater.*, vol. 236, p. 117578, 2020.
[52] A. Laborel-Préneron, J. E. Aubert, C. Magniont, C. Tribout, and A. Bertron, “Plant aggregates and fibers in earth construction materials : a review,” *Constr. Build. Mater.*, vol. 111, pp. 719–734, 2016.
[53] H. Bamogo *et al.*, “Improvement of water resistance and thermal comfort of earth renders by cow dung: an ancestral practice of Burkina Faso,” *J. Cult. Herit.*, vol. 46, pp. 42–51, 2020.
[54] F. Champire, A. Fabbri, J. C. Morel, H. Wong, and F. McGregor, “Impact of relative humidity on the mechanical behavior of compacted earth as a building material,” *Constr. Build. Mater.*, vol. 110, pp. 70–78, 2016.
[55] R. El Nabouche, Q. B. Bui, P. Perrotin, O. Plé, and J.-P. Plassiard, “Numerical modeling of rammed earth constructions: analysis and recommendations,” in *First International Conference on Bio-Based Building Materials*, 2015.
[56] A. Hakimi, N. Yamani, and H. Ouissi, “Rapport : Résultats d’essais de résistance mécanique sur échantillon de terre comprimée,” *Mater. Struct. Constr.*, vol. 29, pp. 600–608, 1996.
[57] V. Y. Chertkov, “The reference shrinkage curve of clay soil,” *Theor. Appl. Fract. Mech.*, vol. 48, pp. 50–67, 2007.
[58] P. Walker and T. Stace, “Properties of some cement stabilised compressed earth blocks and mortars,” *Mater. Struct. Constr.*, vol. 30, pp. 545–551, 1997.
[59] A. Heath, P. Walker, C. Fourie, and M. Lawrence, “Compressive strength of extruded unfired clay masonry units,” *Proc. Inst. Civ. Eng. Constr. Mater.*, vol. 162, no. 3, pp. 105–112, 2009.
[60] M. Bouhicha, F. Aouissi, and S. Kenai, “Performance of composite soil reinforced with barley straw,” *Cem. Concr. Compos.*, vol. 27, pp. 617–621, 2005.
[61] S. Sangma and D. D. Tripura, “Experimental study on shrinkage behaviour of earth walling materials with fibers and stabilizer for cob building,” *Constr. Build. Mater.*, vol. 256, p. 119449, 2020.
[62] S. Goodhew and R. Griffiths, “Sustainable earth walls to meet the building regulations,” *Energy Build.*, vol.

37, pp. 451–459, 2005.
[63] E. Olacia, A. L. Pisello, V. Chiodo, S. Maisano, A. Frazzica, and L. F. Cabeza, “Sustainable adobe bricks with seagrass fibres. Mechanical and thermal properties characterization,” *Constr. Build. Mater.*, vol. 239, 2020.
[64] S. Boussaid, A. El Bakkouri, H. Ezbakhe, T. Ajzoul, and A. El Bouardi, “Comportement thermique de la terre stabilisée au ciment,” *Rev. française Génie Civ.*, vol. 5, no. 4, pp. 505–515, 2001.
[65] A. H. Narayanaswamy, P. Walker, B. . Venkatarama Reddy, A. Heath, and D. Maskell, “Mechanical end thermal properties, and comparative life-cycle impacts, of stabilised earth building products,” *Constr. Build. Mater.*, vol. 243, p. 118096, 2020.
[66] S. Goodhew, R. Griffiths, and L. Watson, “Some preliminary studies of the thermal properties of Devon cob walls.,” in *Terra 2000 8th International Conference on the study and conservation of earthen architecture*, 2000, pp. 139–143.
[67] A. Gimeno-Furio *et al.*, “New coloured coatings to enhance silica sand absorbance for direct particle solar receiver applications,” *Renew. Energy*, vol. 152, pp. 1–8, 2020.
[68] J. Tinsley and S. Pavia, “Thermal performance and fitness of glacial till for rammed earth construction,” *J. Build. Eng.*, vol. 24, p. 100727, 2019.